



# Homogenised model linking microscopic and macroscopic dynamics of a biofilm: Application to growth in a plug flow reactor

Chloé Deygout, Annick Lesne, Fabien Campillo, Alain Rapaport

## ► To cite this version:

Chloé Deygout, Annick Lesne, Fabien Campillo, Alain Rapaport. Homogenised model linking microscopic and macroscopic dynamics of a biofilm: Application to growth in a plug flow reactor. Ecological Modelling, Elsevier, 2013, 250, pp.15-24. 10.1016/j.ecolmodel.2012.10.020 . hal-00604377

**HAL Id: hal-00604377**

**<https://hal.archives-ouvertes.fr/hal-00604377>**

Submitted on 28 Jun 2011

**HAL** is a multi-disciplinary open access archive for the deposit and dissemination of scientific research documents, whether they are published or not. The documents may come from teaching and research institutions in France or abroad, or from public or private research centers.

L'archive ouverte pluridisciplinaire **HAL**, est destinée au dépôt et à la diffusion de documents scientifiques de niveau recherche, publiés ou non, émanant des établissements d'enseignement et de recherche français ou étrangers, des laboratoires publics ou privés.

# A multiscale approach for biofilm modelling: application for growth in a plug flow reactor

C. Deygout<sup>a,b,1,\*</sup>, A. Lesne<sup>c,d</sup>, F. Campillo<sup>a,b</sup>, A. Rapaport<sup>a,b</sup>

<sup>a</sup>*EPI INRA-INRIA MODEMIC (Modelling and Optimisation of the Dynamics of Ecosystems with MICro-organisms). 2 place Pierre Viala, 34060 Montpellier cedex 01, France.*

<sup>b</sup>*UMR INRA-SupAgro 0729 MISTEA (Mathematics, Informatics and STatistics for Environmental and Agronomic Sciences). 2 place Pierre Viala, 34060 Montpellier cedex 01, France.*

<sup>c</sup>*IHÉS (Institut des Hautes Études Scientifiques). 35 Route de Chartres, 91440 Bures-sur-Yvette, France.*

<sup>d</sup>*CNRS UMR 7600 LPTMC (Laboratoire de Physique Théorique de la Matière Condensée). UPMC, 4 place Jussieu, 75252 Paris cedex 05, France.*

---

## Abstract

We propose a new “hybrid” model for the simulation of biofilm growth in a plug flow bioreactor. Our approach consists in combining three scales: a microscopic one for the individual bacteria, a mesoscopic or “coarse-grained” one that homogenises at an intermediate scale the quantities relevant to the attachment/detachment process, and a macroscopic one in terms of substrate concentration. We compare our simulations with the numerical solutions of an existing partial differential equations model at the macroscopic scale.

*Keywords:* biofilm, partial differential equations, individual-based model, plug flow reactor, attachment-detachment, advection-diffusion

---

## 1. Introduction

Biofilms are made of complex communities of micro-organisms attached to a surface. They are ubiquitous structures in nature and in industry, where they can have positive roles such as water treatment or negative roles such as material contamination in industrial processes. In the past years, several modelling approaches were used to represent and study biofilms (see Wang and Zhang 2010 for a general review). One approach is a mathematical description, continuous in time and space, where biofilm development is summed up in a few differential equations (see Wanner et al. 2006; Klapper and Dockery 2010 for reviews), whether ordinary (ODE) or partial (PDE). Using this approach,

---

\*Corresponding author. E-mail: chloe.deygout@gmail.com. Phone: +33140966089.

<sup>1</sup>Present address: Cemagref. UR HBAN (Hydrosystèmes et Bioprocédés). 1 rue Pierre-Gilles de Gennes, CS 10030, 92761 Antony cedex, France.



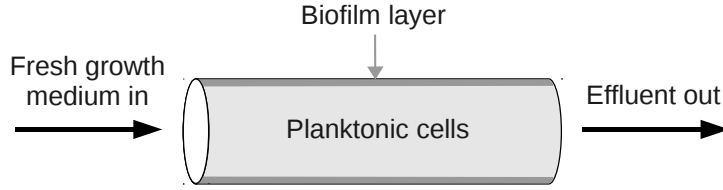


Figure 2: Flow reactor with biofilm.

on a biological system that can be described on three scales spread over this continuum (micro-, meso- and macroscopic). This case study is used to determine the range of validity of our proposed approach. In more complicated situations, where neither a completely microscopic IBM or a PDE system are possible (too many variables or too complicated geometry and boundaries respectively), a mesoscopic approach should prove useful. Also, it should be able to accommodate more easily extensions, such as considering multiple strains in the biofilm.

The biological system we describe is a plug-flow reactor, i.e. a long thin tube fed by a laminar flow (Figure 2). It is well suited to study the use of a coarse-grained description for bacterial growth and detachment, in a case where the hydrodynamical aspects are straightforward. The description is pseudo-1D insofar as diffusion that is transverse to the flow is negligible compared to horizontal advection along the flow and the thickness of the biofilm is not explicitly described.

In the coarse-grained IBM, each bacterium has its own coordinate along the continuous space axis, but this space is also divided in discrete boxes, which are the elements used for the coarse-graining approximations. Inside each box along the tube length, we argue that substrate is uniformly distributed, bacteria reaction rates follow a discretised Monod law, regulation of the attachment of planktonic bacteria is well-accounted for by a logistic curve and the attachment of new bacteria is regulated by another function to be described later on. The use of discretised substrate diffusion and advection (with a discretised gradient and Laplace operator), as well as a discretised Monod law for reaction rates are already common (Picioreanu et al. 1998). The IBM spatial boxes have to be big enough for the law of large numbers to hold inside each box but small enough for our homogeneity assumptions regarding substrate concentration to hold as well (Figure 3).

## 2. Models

### 2.1. Basic hypotheses

Regarding the physical system, we study a plug flow reactor, i.e. a long and thin tube flow reactor as illustrated on Figure 2. A tube with diameter

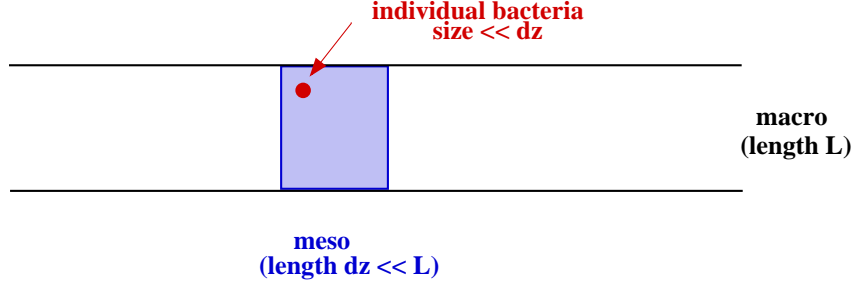


Figure 3: Definition of the different scales.

$D$  extends along the  $z$ -axis, from  $z = 0$  to  $z = L$ . It is fed at  $z = 0$  with growth medium by a laminar flow of fluid in the direction of increasing  $z$  and at velocity  $v$  which is constant. The external feed contains all nutrients in non-limiting amounts except one, which is supplied in a constant, growth-limiting concentration  $s_0$ . The flow carries medium, depleted nutrients, bacteria and their by-products out of the reactor at  $z = L$ . Substrate  $s$  is considered to diffuse with coefficient  $d_s$ . We assume negligible variation of nutrient concentration transverse to the axial direction of the tube, because  $D$  is assumed to be small compared to  $L$ .

Regarding the microbial cells, we consider only one bacterial strain. The bacteria can either be suspended in the fluid or attached to the wall. We consider that planktonic bacteria  $P$  have an unbiased random motility superimposed on the advection mechanism. It is similar to regular diffusion and characterised by a diffusion coefficient  $d_P$ . Attached bacteria  $A$  are assumed to be immobile and there is a finite carrying capacity of the wall for attachment. Planktonic bacteria might attach themselves to the wall depending on surface availability, while attached bacteria might detach themselves from the wall. Also, when attached bacteria divide, their daughter-cells might either attach themselves or become planktonic depending on surface availability.

## 2.2. The Partial Differential Equations

Our reference PDE model is a system of equations developed by Ballyk and Smith (1999). This model is an extension of previous ones describing wall growth in chemostat systems (see Ballyk et al. 2008 for a review of these models) based on the work of Freter et al. (1983) on the mammalian gut. The purpose of the extension by Ballyk and Smith (1999) was to account for spatial heterogeneity and material flow. The model accounts for the concentration of substrate  $s(t, z)$ , the concentration of planktonic bacteria  $c_P(t, z)$  and the concentration of attached bacteria  $c_A(t, z)$ . The latter concentration is measured as a weight

Description	PDE symbol	IBM symbol	Default value
Space	continuous position $z$ [m]	box number $i$ , space step $dz$ [m]	200 boxes
Time [s]	continuous time $t$	discrete time $t$ , time step $dt$	–
Substrate concentration [kg.m <sup>-3</sup> ]	$s(t, z)$	$s_{t,i}$	–
Amount of planktonic bacteria	concentration $c_P(t, z)$ [kg.m <sup>-3</sup> ]	number $N_{P,t,i}$ or mass $m_{P,t,i}$ [kg]	–
Amount of attached bacteria	concentration $c_A(t, z)$ [kg.m <sup>-2</sup> ]	number $N_{A,t,i}$ or mass $m_{A,t,i}$ [kg]	–
Initial substrate concentration	$s_{init}$	$s_{init}$	$1.10^{-3}$ kg.m <sup>-3</sup>
Initial amount of $j$ -type bacteria *1	concentration $c_{j,init}$ [kg.m <sup>-2</sup> ]	number $N_{j,init}$	1000 ind.
Length of tube	$L$	$L$	0.01 m
Diameter of tube	$D$	$D$	$1.10^{-3}$ m
Flow velocity	$v$	$v$	$1.10^{-6}$ m.s <sup>-1</sup>
Conversion yield	$\gamma$	$\gamma$	1
Ratio of tube circumference to cross-sectional area	$\delta$	–	$4.10^3$ m <sup>-1</sup>
Input substrate concentration	$s_0$	$s_0$	$1.10^{-3}$ kg.m <sup>-3</sup>
Attachment rate	$\alpha$	$\alpha$ *2	$1.10^{-8}$ s <sup>-1</sup>
Detachment rate	$\beta$	$\beta$ *2	$1.10^{-5}$ s <sup>-1</sup>
Diffusion rate of substrate	$d_s$	$d_s$ *2	$1.10^{-14}$ m <sup>2</sup> .s <sup>-1</sup>
Diffusion rate of planktonic bacteria	$d_P$	$d_P$ *2	$1.10^{-13}$ m <sup>2</sup> .s <sup>-1</sup>
Maximum growth rate of $j$ -type bacteria *1	$\mu_j$	$\mu_j$ *2	$1.10^{-4}$ s <sup>-1</sup>
Half-saturation constant for $j$ -type bacteria *1	$K_j$	$K_j$ *2	$1.10^{-3}$ kg.m <sup>-3</sup>
Maximum amount of attached bacteria	concentration $c_{A,\infty}$ [kg.m <sup>-2</sup> ]	mass $m_{A,\infty}$ [kg]	$1.10^{-10}$ kg
Wall fraction occupied by attached bacteria	$C_A = c_A/c_{A,\infty}$	$M_A = m_A/m_{A,\infty}$	–
Dimensionless coefficient of $G(C_A)$	$\epsilon$	–	0.01
Fraction of daughters of attached bacteria finding sites on the wall	$G(C_A) = \frac{1-C_A}{1+\epsilon-C_A}$	–	–
Initial individual mass	–	$m_{init}$	$1.10^{-15}$ kg
Mass over which an individual divides	–	$m_{div}$	$2.10^{-15}$ kg

Table 1: Description of the symbols used in both models, with units shown in brackets. Footnotes: \*1  $j = P$  for planktonic bacteria or  $A$  for attached bacteria; here  $P$  and  $A$  parameters have the same values. \*2 Same coefficient in both models but may be used slightly differently to account for discretisation.

per surface unit (not per volume unit like the others) as it represents the surface occupied by the attached bacteria. To convert  $c_A(t, z)$  to the same dimension as  $c_P(t, z)$ , a coefficient called  $\delta$  is used, which is the ratio of the tube surface to the tube volume ( $\delta = \frac{\pi D}{\pi D^2/4} = 4/D$ ).

The equations are the following:

$$\begin{aligned}\frac{\partial s}{\partial t} &= d_s \frac{\partial^2 s}{\partial z^2} - v \frac{\partial s}{\partial z} - c_P f_P(s) \gamma^{-1} - \delta c_A f_A(s) \gamma^{-1} \\ \frac{\partial c_P}{\partial t} &= d_P \frac{\partial^2 c_P}{\partial z^2} - v \frac{\partial c_P}{\partial z} + c_P (f_P(s) - k_P) + \delta c_A f_A(s) (1 - G(C_A)) - \alpha c_P (1 - C_A) + \delta \beta c_A \\ \frac{\partial c_A}{\partial t} &= c_A (f_A(s) G(C_A) - k_A - \beta) + \alpha c_P (1 - C_A) \delta^{-1}\end{aligned}\tag{1}$$

The substrate uptake rates for planktonic and attached bacteria are given by Monod functions:

$$f_j(s) = \frac{\mu_j s}{K_j + s} \text{ where } j = A \text{ or } P\tag{2}$$

The fraction of daughter-cells of attached bacteria finding sites on the wall,  $G(C_A)$ , depends on the amount of surface available for attachment, with  $C_A = c_A/c_{A,\infty}$  being the fraction of surface already occupied. The main biological requirement on this function is to decrease when  $C_A$  increases and reach zero when  $C_A$  is null. The particular function used since the work of Freter et al. (1983) is the following one:

$$G(C_A) = \frac{1 - C_A}{1 + \epsilon - C_A}\tag{3}$$

where  $\epsilon$  is typically small. We also have the following Danckwerts boundary conditions (Dochain and Vanrolleghem 2001):

$$\begin{aligned}vs_0 &= -d_s \frac{\partial s}{\partial z}(0, t) + vs(0, t), & \frac{\partial s}{\partial z}(L, t) &= 0 \\ 0 &= -d_P \frac{\partial c_P}{\partial z}(0, t) + vc_P(0, t), & \frac{\partial c_P}{\partial z}(L, t) &= 0\end{aligned}$$

and the following initial conditions:

$$s(z, 0) = s_{init}(z), \quad c_P(z, 0) = c_{P,init}(z), \quad c_A(z, 0) = c_{A,init}(z), \quad 0 \leq z \leq L$$

These equations lead to two possible steady state regimes: complete washout

of the bacteria from the reactor and successful colonisation of the reactor by the bacteria. Details about these steady states can be found in Ballyk and Smith (1999). In order to study the system more closely, a numerical approach was used to solve it. We used a similar approach as that used by Ballyk and Smith (1999) with a centered second-order finite difference scheme for diffusion, a backward first-order finite difference scheme for advection and the semi-implicit Crank-Nicholson method for time.

### 2.3. The microscopic rules

We are interested in describing attachment processes of our system and understanding the impact and relevance of our description choices. Indeed, studying the results of the PDE system shows that the choice of the  $G$  function for the attachment of daughter-cells of attached bacteria and the attachment/detachment rates have an important impact in defining the location, shape and length of the biofilm. There are two individual-level mechanisms that involve bacterial attachment: attachment of planktonic bacteria and attachment of daughter-cells of attached bacteria.

The space available for attachment is assumed to be limited. The most basic description of these processes on a microscopic scale would be the following: any arriving bacterium attaches itself with probability  $\alpha$  if this bacterium is above or next to an available position, else the bacterium becomes or remains planktonic. This mechanism is the most “microscopic” one we consider, where the complex physical and biological attachment process itself is summed up inside the  $\alpha$  parameter. In order to simplify neighbourhood references, it is possible to homogenise such a mechanism at the mesoscopic scale. Thus, there is no more need to follow exactly the trajectory of each bacterium and check whether the position below it is available or not. Let us consider there are  $X_{max}$  individual positions on the surface in a given neighbourhood, the elementary volume, and already  $X$  individuals occupying some of these positions. A first possibility would be: any arriving bacterium attaches itself with probability  $\alpha$  if there are available positions in the considered space ( $X < X_{max}$ ), else the bacterium becomes or remains planktonic. This “homogenised threshold” mechanism (HT) is the most simple description at the mesoscopic level of an elementary volume, without density-dependence effects. This also means that, using this mechanism assumes bacteria can attach relatively easily, as long as there is some positions available for attachment. Another more complex description would be: any arriving bacterium attaches itself with probability  $\alpha(1 - X/X_{max})$ , which means



that the bacterium becomes or remains planktonic with probability  $\alpha X/X_{max}$ . This “homogenised probability” mechanism (HP) is equivalent to the microscopic mechanism, with regard to the bacteria macroscopic behaviour.

It is interesting to notice that in their equations, Ballyk and Smith (1999) use different mechanisms for the attachment of planktonic bacteria and for the attachment of daughter-cells of attached bacteria. The former is a macroscopic version of the HP mechanism while the latter is of the HT mechanism. These choices are not discussed much in this work nor in their references (Ballyk and Smith 1999). Thus, we have chosen to explore these different mesoscopic mechanisms in our coarse-grained IBM and their impact on model results. Unless specified otherwise, the IBM runs by default with the HT mechanism.

#### *2.4. The coarse-grained Individual-Based Model*

The model description follows the ODD (Overview, Design concepts, Details) protocol for describing individual- and agent-based models (Grimm et al. 2006, 2010). “Overview” is covered in Sections 2.4.1 to 2.4.3, “Design concepts” in Section 2.4.4 and “Details” in Sections 2.4.5 to 2.4.7.

##### *2.4.1. Purpose*

The purpose of this IBM is to represent the biological system described in Section 2.1 while taking into account information from both the macroscopic PDE and a microscopic IBM. We use a “simple” case study to determine the range of validity of this approach.

##### *2.4.2. Entities, macroscopic state variables and scales*

The entities in this model are bacteria. Their microscopic attributes are their position, mass and attachment status. Our main state variables are the number of bacteria in the tube, both attached or detached, as well as the concentration of the substrate. The substrate is not described at a molecular level but its concentration is an attribute of each grid box. The time scale of our simulations is about a few days in duration with a few seconds for the time step. Simulation duration is limited to the time it takes to reach a quasi-steady-state in the system. The time step is constrained by the discretisation scheme used to model the substrate diffusion and advection. The space scale is a few centimetres for the tube length with about 50 micrometers for the space step.

#### 2.4.3. Process overview and scheduling

The first process is substrate reaction-diffusion. The substrate in each grid box diffuses horizontally into the two neighbour boxes (the model being pseudo-1D, we assume homogeneity in the directions transverse to the tube axis) and is advected along the flow into the following box (discretised Laplacian). Bacteria in the box eat one after the other in a random order. The speed with which bacteria eat depends on the local substrate concentration and is given by the Monod law (Eq. 2) as long as substrate is available in the box. The amount eaten by the bacteria increases their mass by that same amount multiplied by the yield factor  $\gamma$ . Substrate concentration in the boxes is updated only at the end of these steps. Despite the artificiality of this sequence, discrepancies should be small because the time step remains very small.

The second process is bacteria division. Bacteria that have a mass higher than the division threshold  $m_{div}$  divide into two bacteria of total mass that of the mother bacteria (see 2.4.7 for details).

The third process is bacteria attachment/detachment. Finally, the detached bacteria are advected by the flow and have a random horizontal motility.

#### 2.4.4. Design concepts

*Basic principles.* This work is based on that of Mabrouk et al. (2010); Mabrouk (2010), itself based on similar assumptions as that of Picioreanu et al. (1998); Kreft et al. (2001). Main differences regard the presence of a flow and taking the border into account.

*Adaptation, objectives, learning, prediction.* Given the small time scale of our simulations, the bacteria in this model do not have adaptive traits and hence do not attempt to meet objectives. They have no learning abilities and do not attempt to predict their future environment.

*Sensing.* The internal variable taken into account by the bacteria is their own mass (which determines division time). The environmental variables taken into account are local substrate concentration (only that of the box in which the bacterium is present), local bacteria abundance (only that of the box in which the bacterium is present) and flow velocity (constant throughout the tube).

*Interaction.* The interactions between the bacteria are only indirect ones, through competition for resources: substrate and attachment sites.

*Stochasticity.* Several events in the model are described with probability rules. When a bacterium divides, the mass and location of the daughter bacteria have a random component (see above). Attachment and detachment are also random (see above).

*Collectives.* When a box reaches its carrying capacity (total attached mass in the box superior or equal to  $m_{A,\infty}$ ), the bacteria form a biofilm on the wall. This can be considered as a collective. Once this collective is formed, new bacteria cannot attach themselves in that box. Nevertheless, this collective is not permanent, and if enough detachment occurs, the mass may again become lower than the threshold  $m_{A,\infty}$ .

*Observation.* Data are collected as the last process in the schedule, for each box. We gather information on substrate concentration, bacteria mass and numbers (both attached or detached), attachment and detachment events.

#### 2.4.5. Initialisation

Before the simulation starts, a number of bacteria are placed in the boxes (location picked from a random uniform distribution), a certain number of which are attached ( $N_{A,init}$ ), the others detached ( $N_{P,init}$ ). Each bacterium has an initial mass of  $m_{init}$ . Substrate is present throughout the tube at a given concentration  $s_{init}$ .

#### 2.4.6. Input data

The input data, such as bacteria initial position, are chosen randomly. Nevertheless, if one wanted to specifically reproduce a given part of a larger tube, initial conditions of the model could be forced to resemble any point of the PDE system representing the whole tube.

#### 2.4.7. Submodels

*Substrate diffusion, advection and reaction.* All these processes are mingled in the model and space is considered sequentially along the flow direction.

1. First, we consider the substrate reaching equilibrium where the flow arrives. Thus, the concentration of substrate in box  $i$ ,  $s_{t,i}$ , increases with substrate arriving by diffusion and advection from the upflow box  $i - 1$  and decreases from substrate leaving by diffusion into box  $i + 1$ .
2. Then, we determine the amount of substrate which is eaten by the bacteria inside box  $i$  (reaction) based on the amount determined in step 1.

3. Finally, we consider the substrate reaching equilibrium where the flows leaves the box. The concentration of substrate in box  $i$  at  $t + dt$ ,  $s_{t+dt,i}$ , is the amount determined in step 2 added with substrate arriving by diffusion from the downflow box  $i + 1$  and once removed substrate leaving by diffusion and advection into box  $i + 1$ .

*Bacterial biology and movement.*

**Growth** Each bacterium consumes a given amount of substrate which is determined by the Monod growth kinetics and its own mass  $m$ . We assume that bacterial growth is directly equal to this amount consumed, multiplied by the conversion yield factor  $\gamma$ . At time  $t$  and in box  $i$ , the increase in mass  $dm$  is the following:

$$dm = \gamma m \frac{\mu_j s_{t,i}}{K_j + s_{t,i}}$$

where  $j$  is either  $A$  or  $P$  for attached or planktonic bacteria respectively (see Table 1 for more details).

**Division** Each bacterium that has a mass higher than the division threshold  $m_{div}$  divides into two bacteria of total mass that of the mother bacterium. Each of the two daughter-bacteria receives half of the mother mass plus or minus a random amount (taken from a uniform distribution between 0 and 25% of the mother mass). One of the daughter bacteria retains the mother location and attachment status, and the other bacterium has the same location plus or minus a random amount (taken from a uniform distribution between 0 and mother diameter). That second daughter bacterium has the same attachment status as its mother by default. If that status is attached, depending on the mechanism used for attachment (see Section 2.3), then the new bacterium might become detached. A daughter bacterium which location is outside the tube is be considered washed out.

**Attachment and detachment** Each of the detached bacteria has a probability involving  $\alpha$  times  $dt$  and  $m_{A,\infty}$  to attach itself on the wall. The exact mechanism can be varied according to the description in Section 2.3. Each of the attached bacteria has a probability  $\beta$  times  $dt$  to detach itself.

**Movement** The detached bacteria are advected by the flow and have a random horizontal motility modelled as a Brownian motion process with an apparent diffusion factor  $d_P$ . The distance crossed over one time step thus follows a Gaussian law of variance twice the diffusion-like factor  $d_P$  multiplied by the time step (Mabrouk 2010).

### 2.5. Numerical experiments

We have run a large number of numerical experiments for both the PDE system and the IBM. Parameter values are those indicated in Table 1 unless mentioned otherwise. In the case of the PDE system, one run gives the deterministic output for a given set of parameters. But in the case of the IBM, several runs were done with different random seeds in order to obtain means of the output variable to represent the average behaviour of the model. Because the stochastic aspects of the IBM are small-scale events, a relatively low number of repetitions was sufficient to average out their effects (a dozen runs). The results we study are: the profiles along the tube for all three variables (in terms of mass, for comparison between the two models), the biofilm length defined as the location along the tube where the difference between two following positions is the largest over the whole profile, and the sum over the whole tube of the attached biomass.

## 3. Results

### 3.1. General description of steady state profiles

In both models, we find similar profiles at the steady state for the default values (Figure 4). These profiles indicate an important development of the biofilm in the leftmost side of the tube where the nutrient flow enters. Parallel to this biofilm development which reaches the carrying capacity, there is an important decrease in substrate concentration. Once a threshold substrate concentration is crossed, there is not enough substrate to allow the growth of a thick biofilm and the amount of attached bacteria reaches a value close to one bacterium along the remainder of the tube. Meanwhile, the amount of detached bacteria increases along the whole tube, these bacteria being released by the thick biofilm of the leftmost part of the tube.

There are nevertheless differences between the two models. First of all, in the right-most part of the tube, there are few attached bacteria and the two models represent this situation differently. The IBM gives a presence-absence

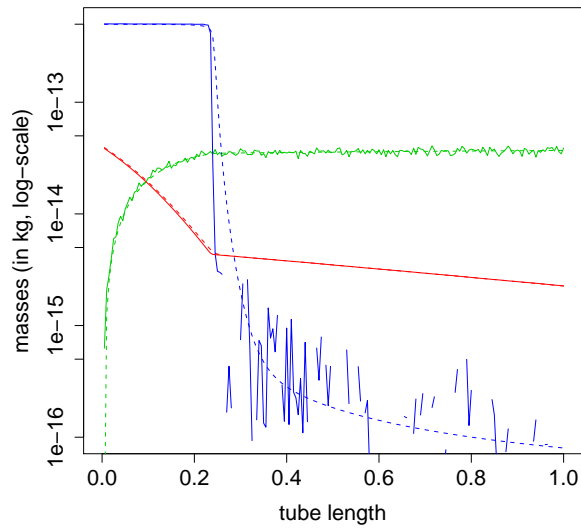


Figure 4: General profile along the tube observed at the steady state for the PDE numerical resolution (dashed lines) and the average over 12 IBM runs (solid lines) with default values as shown in Table 1. The mass of attached bacteria  $m_A$  is represented in blue, the mass of planktonic bacteria  $m_P$  in green and the mass of substrate  $m_S$  in red. The horizontal axis is the length of tube.

information: there is no point in case no attached bacteria are present due to the log-scale of Figure 4. Meanwhile, the PDE gives a continuous expression which in the right-most part of the graph corresponds to about a tenth of an individual bacterium. Nevertheless, both cases give similar values. Second, the attached bacteria in the thick biofilm are slightly more developed in the IBM than in the PDE, which implies a slightly shorter biofilm length. The difference in biofilm length is exaggerated by the log-scale but it remains quite small (about 1 “box” of difference) and the difference in overall attached biomass is about 2%. Finally, there is also the effect of fluctuations in the IBM to be considered. This variability does not reflect individual variance because there has already been some homogenisation but it could be thought of as a “quality” assessment of the coarse-grained IBM. Overall, the variance along the profile is relatively low, in particular for the substrate concentration and the planktonic bacteria. Indeed, these two elements are affected by diffusion processes which smooth their distribution along the tube and there is less variability between runs. For the attached biomass, it is quite low over the thick biofilm length but increases afterwards, in particular over the switch from thick biofilm to almost no attached bacteria (data not shown).

### 3.2. *Parallel between discretisation to solve PDE and discretised events in IBM*

In both cases, whether the model was conceived in a continuous or a discrete manner, the resulting simulations relied on a discretised code. Thus, in both cases, we can compare the impact of the number of spatial boxes making up the whole tube. By keeping the tube length constant and increasing the number of boxes, the size and volume of each box is reduced. Using a large number of boxes increases the similarity of the results with those that might be obtained with a continuous representation. But it also increases simulation run time and it reduces the number of individuals or biomass present in each box which may lead to observing quantities smaller than one individual in the case of the PDE system. In this work, we find that the numerical experiments are relatively resilient to the number of boxes and thus to box size as well (Figure 5). By using a small number of boxes, there is a slight tendency to overestimate the biofilm length in both models, but the difference remains well under 1%.

### 3.3. *Sensitivity analysis*

Overall, the same effects are observed on PDE and IBM simulations. Differences in the main results (length of biofilm, mass of attached bacteria) between

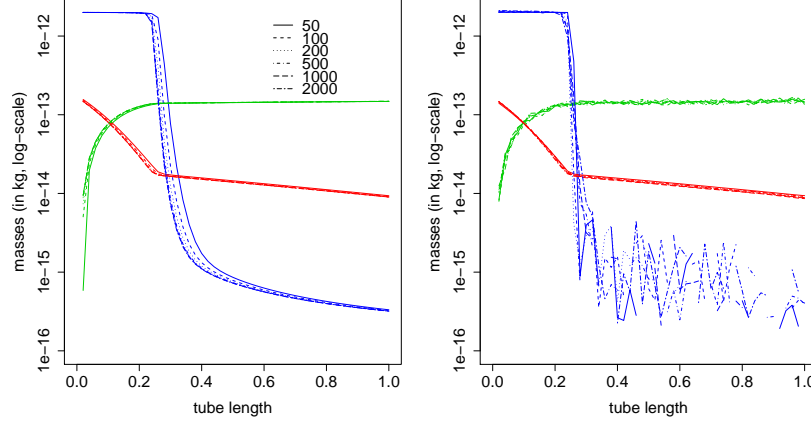


Figure 5: Effect of the number of boxes on the steady state profile for (a) the PDE numerical resolution and (b) the average over ... IBM runs. The mass of attached bacteria  $m_A$  is represented in blue, the mass of planktonic bacteria  $m_P$  in green and the mass of substrate  $m_S$  in red. The horizontal axis is the box coordinate along the tube divided by the number of boxes in order to compare between cases.

the two models remained well under 5%. The parameters tested here are those which have a major impact on the results.

An increase in  $s_0$  leads to an increase in the length of biofilm formed (Figure 6). An increase in  $v$  leads to a similar effect. Indeed, increasing  $v$  leads to an increased amount of substrate available for the bacteria.

An increase in both  $\mu_j$  or both  $K_j$  leads first to an increase in the length of biofilm formed and after reaching a peak value it leads to a decrease (Figure 7). Indeed, for low values of  $\mu_j$ , bacteria are washed out while for high values of  $\mu_j$ , the bacteria are very efficient in eating the substrate and only a short length of biofilm can develop before the tube is emptied of substrate. Thus, it is for intermediate values of  $\mu_j$  that a maximum length of biofilm is observed. Similar results are observed for  $K_j$  but with high values of  $K_j$  leading to a wash-out and low values of  $K_j$  leading to a short and efficient biofilm.

An increase in  $m_{A,\infty}$  leads to a decrease in the length of biofilm which is formed (Figure 8). Indeed, since the biofilm is thicker, the substrate is completely eaten earlier along the tube and prevents further biofilm development.

An increase in  $\alpha$  has very little effect on the development of the main biofilm in the leftmost part of the tube. Nevertheless, it leads to an increase in the



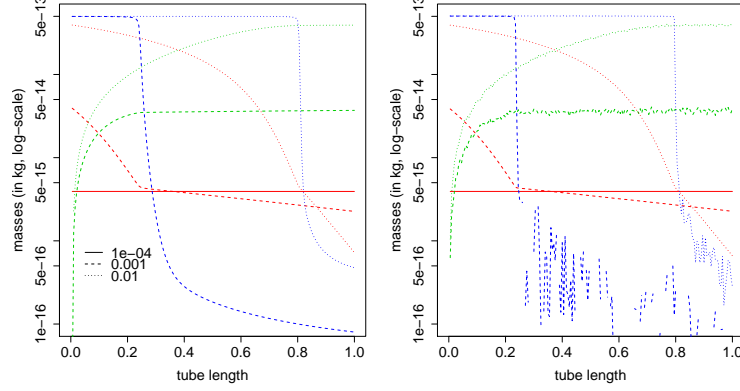


Figure 6: Effect of the input concentration of substrate  $s_0$  on the steady state profile for (a) the PDE numerical resolution and (b) the average over 12 IBM runs. The mass of attached bacteria  $m_A$  is represented in blue, the mass of planktonic bacteria  $m_P$  in green and the mass of substrate  $m_S$  in red. The horizontal axis is the length of tube.

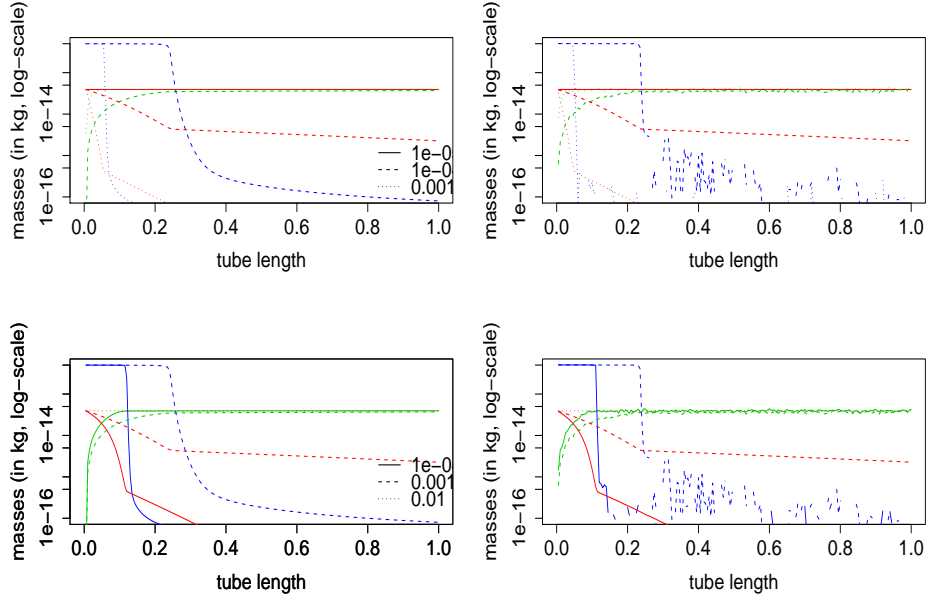


Figure 7: Effect of (i) both  $\mu_j$  or (ii) both  $K_j$  on the steady state profile for (a) the PDE numerical resolution and (b) the average over 12 IBM runs. The mass of attached bacteria  $m_A$  is represented in blue, the mass of planktonic bacteria  $m_P$  in green and the mass of substrate  $m_S$  in red. The horizontal axis is the length of tube.

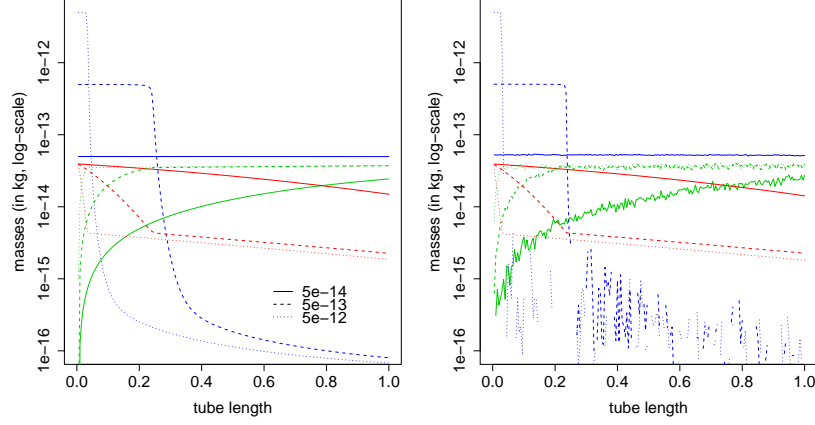


Figure 8: Effect of  $m_{A,\infty}$  on the steady state profile for (a) the PDE numerical resolution and (b) the average over 12 IBM runs. The mass of attached bacteria  $m_A$  is represented in blue, the mass of planktonic bacteria  $m_P$  in green and the mass of substrate  $m_S$  in red. The horizontal axis is the length of tube.

development of the biofilm in the rest of the tube (Figure 9). Bacteria in this part of the biofilm do not grow because there is very little substrate left but the biofilm is built via attachment of planktonic bacteria flowing by. An increase in  $\beta$  leads to a decrease in the length of biofilm formed (Figure 9). Indeed, for large values of  $\beta$ , the amount of substrate needed for biofilm development (including compensation for biofilm detachment) is higher than for smaller values of  $\beta$ . For a large enough value of  $\beta$ , there is wash-out.

### 3.4. Impact of microscopic attachment mechanisms

Different attachment mechanisms were considered (Figure 10). The PDE mechanism of the G function and the “homogenised threshold” (HT) mechanism lead to similar macroscopic behaviours, with an abrupt limit to attachment possibilities for bacteria and thus an abrupt distinction between a part of the tube with a thick biofilm and the other part with almost no attached bacteria. Whichever mechanism is followed for the attachment of planktonic bacteria, the results are similar because this attachment is mostly important in the part of the tube with little attached bacteria and thus for values where all mechanisms behave similarly. On the other hand, whether the attachment of daughter bacteria follows the HT or the HP mechanism has a much more important impact

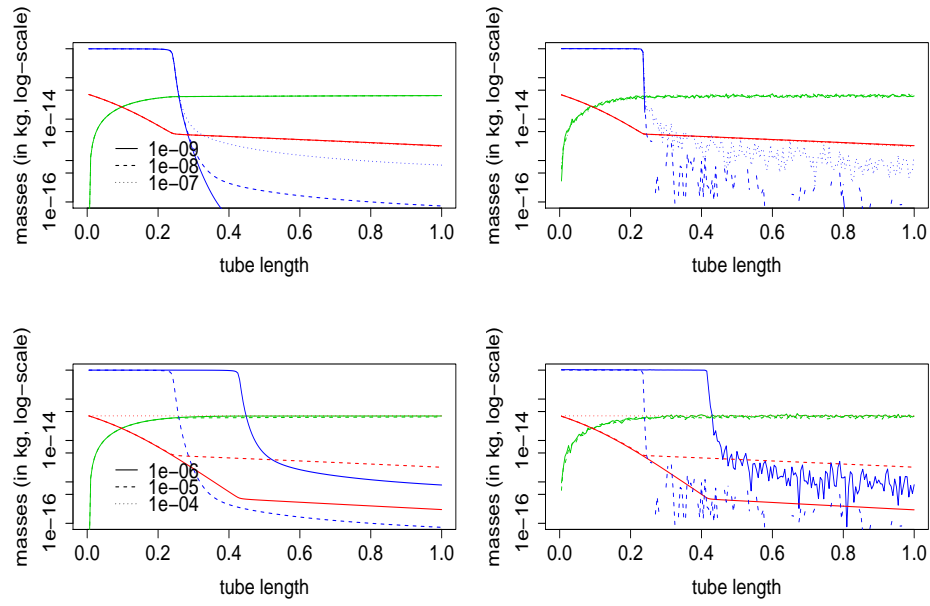


Figure 9: Effect of (i)  $\alpha$  and (ii)  $\beta$  on the steady state profile for (a) the PDE numerical resolution and (b) the average over 12 IBM runs. The mass of attached bacteria  $m_A$  is represented in blue, the mass of planktonic bacteria  $m_P$  in green and the mass of substrate  $m_S$  in red. The horizontal axis is the length of tube.

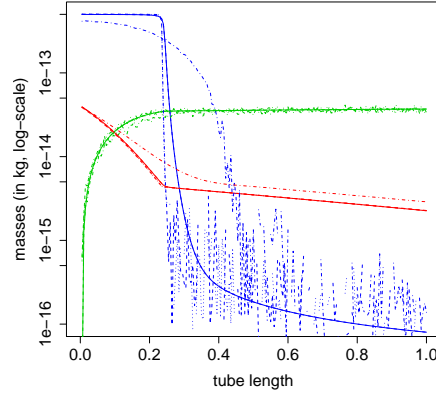


Figure 10: Comparison of different mechanisms for the attachment of bacteria in the IBM (various dashed and dotted lines) with the reference PDE (solid lines) at the steady state. In the IBM, the PDE mechanism of the G function and the “homogenised threshold” (HT) mechanism give similar results whether used for the attachment of planktonic or daughter bacteria and their results are thus both represented by the dotted lines. The dashed lines represent the use of the “homogenised threshold” (HT) mechanism for the attachment of daughter bacteria and of the “homogenised probability” (HP) for the attachment of planktonic bacteria in the IBM. The dash-dot lines represent the use of the “homogenised probability” (HP) mechanism for both kinds of attachment in the IBM. The mass of attached bacteria  $m_A$  is represented in blue, the mass of planktonic bacteria  $m_P$  in green and the mass of substrate  $m_S$  in red. The horizontal axis is the length of tube.

on the overall profile along the tube. Indeed, the “homogenised probability” (HP) mechanism leads to a much smoother transition between the part of the tube with a thick biofilm and the other part with almost no attached bacteria. It remains to be seen which may be the more realistic approach.

## 4. Discussion

### 4.1. Modelling choices

First of all, our model represents a 3-dimensional system in a pseudo-1-dimensional manner. We take only the coordinate along the tube axis (z-axis) into account, assuming that at a given z-coordinate substrate concentration is homogeneous inside the tube and that the precise location of bacteria is much less important than whether they are attached or planktonic. In general, it has been observed that minimal models offer an interesting trade-off between realism and generality.

In this work we have built an IBM with the aim to represent a given biological system and then justify choices made in the pre-existing PDE system. In order to build the IBM, a number of elements could not be derived straightforwardly. For example, all kinds of stochastic events had to be added, in particular regarding the division mechanism. We chose to use individual mass as a non-stochastic indicator of division time, but the distribution of this mass between the two daughter bacteria had a stochastic component. This simple mechanism proved sufficient to prevent any synchronisation among the bacteria and thus more complex ones were not used in the IBM.

An important part of this work relied on the study of attachment patterns and various mechanisms were proposed both for attachment of planktonic bacteria and daughters of attached bacteria. Following the equation system, we studied both kinds of attachment separately. Nevertheless, one might wonder whether it is relevant to distinguish between them. Thus, we might suggest using the same mechanism for both, keeping in mind that in this particular system the precise mechanism behind the attachment of planktonic bacteria has a much minor effect than that of the daughters of attached bacteria.

### 4.2. Perspectives

Using an IBM approach to describe this plug-flow system has several advantages. First of all, it allows us to use “biological” rules, i.e. rules that can intuitively be suggested (and tested) by biologists based on their in-depth

knowledge of the real system. This makes the system more amenable to interactions with experiments and also to changes in the choice of mechanisms. This IBM may thus lead to improvement over the original model proposed by Freter et al. (1983) and its variations (Ballyk and Smith 1999) by allowing us to test mechanisms that could not be easily formulated or even solved analytically. One possibility would be to explore the biofilm dynamics when considering different bacterial strains competing inside the tube for space and/or substrate resources. Also, we could consider taking into account the (transversally) inhomogeneous velocity profile through a shear rate, generating a shear force on attached bacteria which would promote their detachment (with an effect on the  $\beta$  parameter) and limit the thickness of biofilm (effect on the  $c_{A,\infty}$  carrying capacity parameter).

Regarding the density issue (thick biofilm in one part of the tube, few attached bacteria in the other part), we could consider an association of the different models. Indeed, currently we have compared the PDE and IBM models but a prospect could be to use them sequentially with the PDE at the start of the tube where the population is larger and a transition to the IBM for the rest of the tube where the population is smaller.

Finally, with this coarse-grained IBM, we open discussions on top-down interactions (macroscopic constraints on individual bacteria or mesoscopic boxes, feedbacks) and on bottom-up interactions (emergent collective features).

#### 4.3. Conclusion

We have proposed a new multiscale model of biofilm growth in a plug flow reactor, with reasonable runtimes for the simulations while remaining close to microscopic processes and knowledge. In particular, our approach focuses on the hypotheses regarding the attachment/detachment process that is at the core of biofilm growth. The comparison with the PDE model has led to similar steady-state concentration profiles at the macroscopic level, justifying qualitatively the attachment/detachment terms introduced at the mesoscopic scale, although some differences could be observed. An IBM approach such as the one we use provides additional information on second-order terms or variance around the average profile that have been compared with the PDE model. Our framework is suitable for extensions to multi-species biofilm or more complex interactions between individuals.

## Acknowledgments

This work has been achieved within the DISCO (“multi-scale modelling bio-Diversity Structure COupling in biofilms”) project of the French Agency of Research SYSCOMM program (ANR AAP215-SYSCOMM-2009), that has financed CD’s postdoctoral fellowship.

## References

- M. Ballyk and H. L. Smith. A model of microbial growth in a plug flow reactor with wall attachment. *Mathematical Biosciences*, 158(2):95–126, 1999. doi: 10.1016/S0025-5564(99)00006-1.
- M. Ballyk, D. Jones, and H. L. Smith. The biofilm model of Freter: a review. In *Structured population models in biology and epidemiology*, pages 265–302. P. Magal and S. Ruan, Springer edition, 2008.
- D. Dochain and P. Vanrolleghem. *Dynamical modelling and estimation in wastewater treatment processes*. 2001.
- R. Duddu, D. L. Chopp, and B. Moran. A two-dimensional continuum model of biofilm growth incorporating fluid flow and shear stress based detachment. *Biotechnology and Bioengineering*, 103(1):92–104, 2009. doi: 10.1002/bit.22233.
- H. J. Eberl, D. F. Parker, and M. C. M. Vanloosdrecht. A new deterministic spatio-temporal continuum model for biofilm development. *Journal of Theoretical Medicine*, 3(3):161–175, 2001. doi: 10.1080/10273660108833072.
- R. Freter, H. Brickner, J. Fekete, M. M. Vickerman, and K. E. Carey. Survival and implantation of escherichia coli in the intestinal tract. *Infection and Immunity*, 39(2):686–703, 1983.
- V. Grimm, U. Berger, F. Bastiansen, S. Eliassen, V. Ginot, J. Giske, J. Goss-Custard, T. Grand, S. K. Heinz, G. Huse, A. Huth, J. U. Jepsen, C. Jrgensen, W. M. Mooij, B. Mller, G. Pe’er, C. Piou, S. F. Railsback, A. M. Robbins, M. M. Robbins, E. Rossmanith, N. Rger, E. Strand, S. Souissi, R. A. Stillman, R. Vab, U. Visser, and D. L. DeAngelis. A standard protocol for describing individual-based and agent-based models. *Ecological Modelling*, 198(1-2):115–126, 2006. doi: 10.1016/j.ecolmodel.2006.04.023.

- V. Grimm, U. Berger, D. L. DeAngelis, J. G. Polhill, J. Giske, and S. F. Railsback. The ODD protocol: A review and first update. *Ecological Modelling*, 221(23):2760–2768, 2010. doi: 10.1016/j.ecolmodel.2010.08.019.
- F. L. Hellweger and V. Bucci. A bunch of tiny individuals - individual-based modeling for microbes. *Ecological Modelling*, 220(1):8–22, 2009. doi: 10.1016/j.ecolmodel.2008.09.004.
- I. Klapper and J. Dockery. Mathematical description of microbial biofilms. *SIAM Review*, 52(2):221–265, 2010. doi: 10.1137/080739720.
- J.-U. Kreft, C. Picioreanu, J. W. T. Wimpenny, and M. C. M. van Loosdrecht. Individual-based modelling of biofilms. *Microbiology*, 147:2897–2912, 2001.
- C. S. Laspidou, A. Kungolos, and P. Samaras. Cellular-automata and individual-based approaches for the modeling of biofilm structures: Pros and cons. *Desalination*, 250(1):390–394, 2010. doi: 10.1016/j.desal.2009.09.062.
- N. Mabrouk. *Analyzing individual-based models of microbial systems*. PhD thesis, Université Blaise Pascal de Clermont-Ferrand, 2010.
- N. Mabrouk, G. Deffuant, T. Tolker-Nielsen, and C. Lobry. Bacteria can form interconnected microcolonies when a self-excreted product reduces their surface motility: evidence from individual-based model simulations. *Theory in Biosciences*, 129(1):1–13, 2010. doi: 10.1007/s12064-009-0078-8.
- C. Picioreanu, M. C. M. van Loosdrecht, and J. J. Heijnen. A new combined differential-discrete cellular automaton approach for biofilm modeling: application for growth in gel beads. *Biotechnology and Bioengineering*, 57(6):718–731, 1998.
- Q. Wang and T. Zhang. Review of mathematical models for biofilms. *Solid State Communications*, 150(21-22):1009–1022, 2010. doi: 10.1016/j.ssc.2010.01.021.
- O. Wanner, H. J. Eberl, E. Morgenroth, D. Noguera, C. Picioreanu, B. Rittmann, and M. C. M. van Loosdrecht. *Mathematical modeling of biofilms*. IWA publishing edition, 2006.